Improvement of the Anticancer Activities of Telmisartan by Zn(II) Complexation and Mechanisms of Action

Valeria R. Martínez, María V. Aguirre, Juan S. Todaro, Evelina G. Ferrer & Patricia A. M. Williams

Biological Trace Element Research

ISSN 0163-4984

Biol Trace Elem Res
DOI 10.1007/s12011-019-02013-w

Springer

Biological Trace Element Research
https://doi.org/10.1007/s12011-019-02013-w

Improvement of the Anticancer Activities of Telmisartan by Zn(II) Complexation and Mechanisms of Action

Valeria R. Martínez[1] · María V. Aguirre[2] · Juan S. Todaro[2] · Evelina G. Ferrer[1] · Patricia A. M. Williams[1]

Received: 18 September 2019 / Accepted: 9 December 2019

Abstract

To improve the anticancer activity of telmisartan, its structure has been modified by Zn(II) complexation giving $[Zn(Telm)_2(H_2O)_2]\cdot 2H_2O$ (ZnTelm). The cytotoxic effect was measured on the human lung cancer cells (A549) and on the lung fibroblast cells (MRC-5). The complex markedly improved anticancer activity (IC_{50} 75 μM) of telmisartan (IC_{50} 125 μM) or $ZnSO_4$ (IC_{50} 225 μM) and did not show toxicity on non-cancer cells, inducing oxidative stress with cellular ROS generation and GSH/GSSG decrease. Apoptosis was the dominant form of cell death for the complex. The Bax/Bcl-XL ratio was significantly increased as well as caspase-3 activation. Both the complex and the ligand bind to bovine serum albumin (BSA) and can be stored and transported by the protein but the interaction with the complex is greater. Telmisartan binds BSA by hydrophobic interactions while the interaction of ZnTelm occurs through van der Waals forces and hydrogen bonding. Therefore, it can be shown that the coordination complex ZnTelm improved the anticancer activity of the antihypertensive drug telmisartan (IC_{50} 75 μM and 125 μM, respectively) and the interaction with BSA.

Keywords Telmisartan · Zn(II) metal complex · Cancer · Bovine serum albumin

Introduction

Telmisartan, a member of the Angiotensin II receptor blockers (ARBs), is an effective antihypertensive compound which has stronger affinity to bind the AT1 receptor site [1]. Furthermore, several reports have demonstrated that telmisartan has the capacity to exert cytotoxic effects in human lung adenocarcinoma A549 cell line [2] as well as apoptosis induction, ROS generation, and autophagy flux inhibition [3, 4]. Telmisartan (Fig. 1) is a flexible ligand with four nitrogen atoms in the benzimidazole groups and two oxygen atoms in the carboxylic acid group that ensures diverse binding modes.

The essential trace element zinc is related to multiple biological processes including catalytic, regulatory, and structural. It also participates in reproduction, cell proliferation, and systems of defense against ROS [5, 6]. Dietary deficiencies of zinc can increase oxidative injury compromising DNA repair mechanisms, promoting DNA damage [7, 8] and therefore they are associated to cancer.

Previous reports on the interaction of Zn(II) with telmisartan showed two compounds a coordination Zn-Cu complex, $[Zn_{1.6}Cu_{6.4}Telm_{16}]$, that was obtained by cation exchange from $[Cu_8Telm_{16}]$ [9] and a zinc salt of telmisartan that has been synthesized in the form of the ionic salt, $Zn(Telm)_2$ [10]. The salt improved some physicochemical and pharmaceutical properties of the drug but the spectroscopic characterization and the evaluation of its mechanism of action in cancer cells were not reported. In the present study, we have designed and characterized a coordination compound between Zn(II) and telmisartan and evaluated it as a potential anticancer compound against human lung adenocarcinoma A549 cells and determined the mechanisms of action and its selectivity against embryonic human lung fibroblasts MRC-5 cell line. To ascertain the transport and delivery in plasma, the interactions of the compounds with BSA were determined.

Electronic supplementary material The online version of this article (https://doi.org/10.1007/s12011-019-02013-w) contains supplementary material, which is available to authorized users.

✉ Patricia A. M. Williams
williams@quimica.unlp.edu.ar

[1] Centro de Química Inorgánica (CEQUINOR-CONICET-CICPBA-UNLP), 120 N° 1465, La Plata, Argentina

[2] Laboratorio de Investigaciones Bioquímicas. Facultad de Medicina. UNNE, Moreno 1240, Corrientes, Argentina

Published online: 20 December 2019

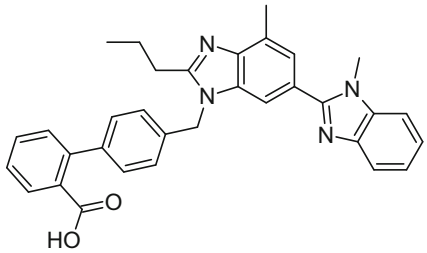

Fig. 1 Structure of telmisartan

Experimental

Materials and Methods

Biopack (Argentina) and Rundu Pharma (Shangai, China) supplied Zinc(II) chloride (97% purity) and telmisartan, respectively. The reagents and solvents used were of analytical grade. For the measurement of the infrared spectra (IR) of the solids, a Bruker IFS 66 FTIR spectrophotometer in KBr pellets in a range from 4000 to 400 nm was used. A Shimadzu system (model TG-50) was used for the thermogravimetric (TGA) analyses, at a heating rate of 10 °C min^{-1} and constant oxygen flow of 50 mL min^{-1}. A Carlo Erba EA 1108 analyzer was used for the determination of elemental analyses for C, H, and N. Electronic and fluorescence spectra were recorded in a Hewlett-Packard 8453 diode-array and a Shimadzu RF-6000 spectrophotometer, respectively. Zn content determination was carried out by atomic absorption spectrometry. A Bruker Ultrashield 600, 14.1 Tesla spectrometer was used for ^{1}H and ^{13}C NMR measurements, working with 100% DMSO-d6 solution (0.01 M concentrations) at 25 °C. Tetramethylsilane was used as internal standard for calibrating chemical shift δ.

Synthesis of $[Zn(Telm)_2(H_2O)_2]\cdot 2H_2O$

A 10-mL solution of telmisartan (0.2 mmol, 0.102 g), in 96% ethanol at pH 7 (adjusted by the addition of aqueous solution 1 M NaOH), was stirred at 70 °C. Then, a solution of $ZnCl_2$ (0.1 mmol, 0.013 g) in 5 mL of ethanol was added dropwise. The resulting solution was left at ambient temperature, and upon 24 h evaporation, a white powder was obtained. The solid was filtered over a glass filter, washed with hot ethanol, and air-dried. Elemental analysis (%): Calc for $C_{66}H_{66}N_8O_8Zn$: C, 68.0; H, 5.6; N, 9.7; Zn, 5.7. Found: C, 67.8; H, 5.4; N, 9.5; Zn, 5.5. TGA measurements showed two labile water molecules that were lost at 60 °C (% calc, 3.1; % exp. 3.0). The next step at 226 °C (% calc, 3.1; % exp. 2.9) was consistent with the loss of two coordinated water molecules. UV-Vis (DMSO): 297 nm. Photoluminescence properties: λ_{ex} 343 nm; λ_{em}: 381 nm (telm); λ_{em} 383 nm (ZnTelm). ^{1}H NMR (600 MHz, DMSO-d6) (δ ppm): 0.97(s, 3H), 1.79(s, 2H), 2.56 (s, 3H), 2.89(s, 3H), 3.35 (m, 8H), 3.70 (s, 3H), 5.44(s, 2H), 7.01–7.69 (m, 14H). ^{13}C NMR (150 MHz, DMSO-d6) (δ ppm): 14.27, 16.86, 21.24, 29.18, 32.06, 46.88, 111, 111.1, 119.1, 122.19, 122.98, 123.53, 126.66, 127.10, 128.58, 129, 129.13, 129.25, 129.97, 134.97, 135.11, 139.5, 141.46, 143.36, 154.81, 156, 173.87. FTIR: C=O (CCOH in Tlm, 1696 cm^{-1}) splits into $\nu_{as}(COO^{-})$ 1592 cm^{-1} and $\nu_{s}(COO^{-})$1400 cm^{-1} in ZnTelm (monodentate coordination).

Cell Culture Techniques

A549 cells (human lung carcinoma) and MRC-5 cells (embryonic human lung fibroblasts) were used for testing the anticancer activities of the compounds. The cells were transferred into 6- or 48-well plates (2×10^6 cells mL^{-1}), and after 24 h, they were grown to 85–90% confluency in Dulbecco's modified Eagle's medium (DMEM, Gibco/BRL) supplemented with 10% fetal bovine serum (FBS, Internegocios SA). Solutions of $ZnSO_4$, telmisartan and ZnTelm dissolved in 2.5 μL DMSO plus 500 μL DMEM without FBS were added to each well in order to obtain a final concentration between 0 and 100 μM.

Anticancer Activity

Cell Viability Assay, ROS Generation, GSH Levels, and GSG/GSSG Ratio

After 24 h incubation with the compounds, the cytotoxicity was tested by the MTT (3-(4,5-dimethylthiazol-2-yl)-2,5-diphenyltetrazolium bromide, Abcam, Cambridge, UK) assay. Cells were incubated with 250 μL of the solution, followed by 3 h incubation. Then, DMSO was added into each well to dissolve the purple formazan crystals. The optical density was measured at 560 nm.

The intracellular ROS were detected using the H_2DCFDA probe (2,7-dichlorodihydrofluorescein diacetate). After 24 h incubation with the complex, telmisartan and $ZnSO_4$, A549 cells were incubated for 90 min with 10 μM H_2DCFDA (Merck, Darmstadt, Germany) at 37 °C in the dark. Subsequently, the cells were collected and lysed in 0.1% Triton X-100 solution (Biopack, Argentina). The intracellular ROS were detected by spectrofluorometry (λ_{exc} = 485 nm and λ_{em} = 520 nm).

The GSH levels and GSH/GSSG ratio were measured with a spectrofluorometer using the modified Hissin and Hilf's method [11]. For GSSG measurements and to mask GSH contents, 100 μL cellular aliquots were incubated with 0.04 M of N-ethylmaleimide (NEM, after 24 h incubation with the compounds), then NaOH (1.8 mL, 0.1 M, pH 12) was added to hydrolyze GSSG, and a final

addition of 0.1% methanolic solution of *o*-phthaldialdehyde (OPT) was carried out. For GSH measurements, 100 μL aliquots of lysed cells were mixed with 1.8 mL of phosphate buffer (Na_2HPO_4 0.1 M-EDTA 0.005 M, pH 8, ice-cold) and 100 μL of 0.1% OPT were added. Fluorescence measurements were performed at 420 nm ($\lambda_{exc} = 350$ nm). Protein content was estimated using the Bradford technique [12]. Calibration curves using GSH and GSSG as standard solutions (Sigma-Aldrich) were used to calculate the microgram GSH/milligram protein ratio. The ratio was expressed as percentage of the control.

Apoptosis, Fluorescence Microscopy, and Western Blotting Assay

The cellular and nuclear morphological alterations of the A549 cells were confirmed by fluorescence microscopy with acridine orange (AO) and ethidium bromide (EB) staining procedure [13]. In 35-mm Petri dish, 2×10^6 cells mL^{-1} were cultured and after 24 h incubation, 75 μM of $ZnSO_4$, telmisartan, and ZnTelm were added. For the negative control, 0.5% of DMSO and, for the positive control, 1% of H_2O_2 were added. After 24 h, the medium with the detached cells was collected, the adherent cells were raised off with TrypLE express (Gibco) and both liquids were centrifuged. The pellet was suspended in 1 mg mL^{-1} AO/EB in PBS solution for 10 min. The cell morphologies were analyzed under an inverted fluorescence microscope Olympus CX-35.

The effects of $ZnSO_4$, telmisartan, and ZnTelm on Bax, Bcl-XL, and caspase-9 expression were observed by Western blotting analysis. A549 cells were cultured with 75 μM (IC_{50} of the complex) concentration of the compounds for 24 h. The cells were suspended in RIPA lysis buffer (pH 7.4, 50 mM Tris, 2.5 mg mL^{-1} deoxycholic acid, 10 μg mL^{-1} Nonidet-40, 150 mM NaCl, 1 mM EGTA), containing the protease inhibitors cocktail: 0.95 μg mL^{-1} aprotinin, 2.5 μg mL^{-1} leupeptin, and 2.5 mM phenylmethylsulfonyl fluoride (pH 7.4). Then, the isolated proteins were transferred to nitrocellulose membranes at 50 V for 2 h. Membranes were blocked followed by overnight incubation at 4 °C with the corresponding primary antibody anti-β actin (1/750, Sigma-Aldrich) to normalize the blottings, anti-Bax (1/750), anti-Bcl-XL (1/1000), and Caspase-9 (1/750) (Santa Cruz Biotechnology, CA, USA) and secondary antibody (1:1000) (Jackson Immunoresearch Inc., USA) conjugated to horseradish peroxidase in 5% skim milk for 1 h at 4 °C. An Opti4CN kit (Bio-Rad, CA, USA) was used to detect the bands of interest and they were analyzed using ImageJ software. To express the results, the ratio (protein of interest OD/β-actin OD) × 100 was determined.

BSA Interaction

Because the intrinsic fluorescence of telmisartan and ZnTelm (360 and 368 nm, respectively) appeared in the same spectral region of that of BSA, the quenching measurements were performed at fixed concentrations of the ligand and complex and variable BSA concentrations. BSA solutions were prepared dissolving the albumin in Tris-HCl buffer (0.1 M, pH 7.4) to attain final concentrations of 0, 2, 6, 10, 20, and 30 μM. Solutions of telmisartan and ZnTelm in DMSO were added to the BSA solution at final concentrations of 10 μM and incubated at 298 and 310 K for 1 h. The fluorescence spectra were measured at $\lambda_{exc} = 280$ nm and $\lambda_{em} = 290$–450 nm with spectral bandwidths of at 10 nm. The spectra were deconvolved by the curve-fitting method with the Levenberg–Marquardt algorithm. The OriginPro 9.1.0 (OriginLab Corporation, Northampton, USA) software was used for the baseline corrections, normalization, curve-fitting and calculations.

Statistical Analysis

All the data represent the mean ± standard error of the mean (SEM) of results obtained from at least three independent experiments, and each was performed by triplicate. Statistical analysis was performed by one-way ANOVA test followed by Fisher's test using the OriginPro 9.1.0 (OriginLab Corporation, Northampton, USA) software. $p < 0.05$ values were considered statistically significant.

Results

Spectral Characterization

According to the elemental analysis of ZnTelm and the thermal measurements, a L:M 2:1 stoichiometry for $[Zn(Telm)_2(H_2O)_2].2H_2O$ has been suggested. The assignment of the FTIR vibration spectral bands of telmisartan and its Zinc(II) complex (Table S1) was performed by comparison with previous data of telmisartan and its copper complex [14]. The $\Delta(COO^-)$ value for the complex (192 cm^{-1}) indicated that the carboxylate moiety binds to the metal center in a monodentate mode. The reduction in the intensity of the spectral modes related to the O–H group of the –COOH group indicated the deprotonation and/or coordination of the ligand, suggesting that telmisartan bound to the metal ion through the carboxylate (COO^-) group. Similar results have previously been obtained for the telmisartan complexes of Y(III) and Nd(III) [15]. The chemical shifts in the ^{1}H-NMR spectrum of the complex (Fig. S1) are similar to those of telmisartan [16, 17] but showed the disappearance of the signal due to the carboxylic acid proton, indicating, again the –COOH

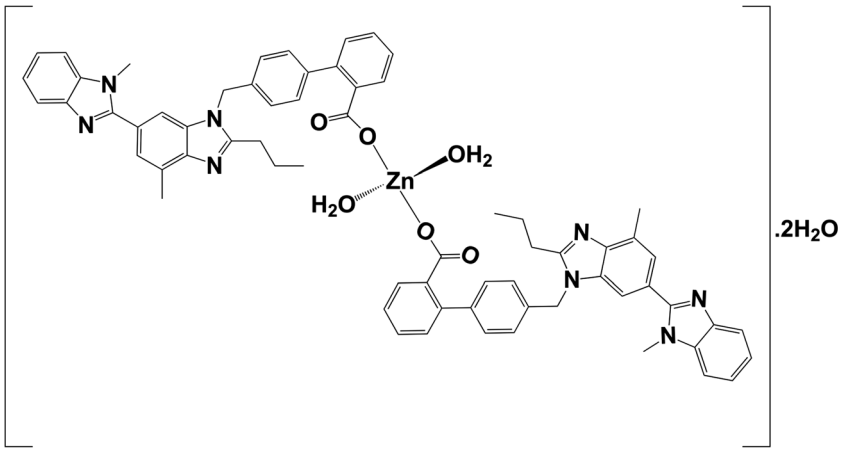

Fig. 2 Proposed structure for ZnTelm

deprotonation during the complex formation. The broad singlet at δ 3.35 ppm has been assigned to coordinated water. The ^{13}C NMR spectral data for the Zn complex revealed that the –COOH signal was shifted downfield upon complexation, due to the bonding of the oxygen atom of the carboxylate group of telmisartan with Zn(II). Therefore, the experimental results using two spectroscopic techniques indicated that the Zn(II) ion interacted with telmisartan trough the aromatic carboxylate of the ligand (Fig. 2).

Anticancer, Oxidative Stress, Apoptosis

The cytotoxicity of $ZnSO_4$, telmisartan, ZnTelm, A549, and MRC-5 cell line was investigated by the MTT assay. Results were expressed as percent with respect to basal values. Figure 3 a shows that $ZnSO_4$ did not exert deleterious effects on A549 cells while telmisartan only exerted significant toxicity at high concentrations (100 μM). The complex significantly induced cell death on A549 cells in dose dependent response ($IC_{50} = 75 \pm 8.1$ μM). The data are consistent with previous investigations on telmisartan that has shown to be mildly toxic in A549 cell line by MTT assay after 24 h exposure, with a ca. 40% reduction on cell viability at 50 μM [2, 18]. The MTT assay performed on the MRC-5 cells revealed that at low doses of $ZnSO_4$, the cell proliferation increased up to 25 μM, and then the viability slowly decreases. Telmisartan did not exert toxic behavior on the MRC-5 cells (Fig. 3b), like the previous effects found for normal fibroblasts [18]. Cell viability upon incubation of the complex in the MRC-5 cell line resulted slightly affected suggesting that ZnTelm has the ability to target selectively the A549 cancer cells.

To evaluate if the toxic mechanism of action occurs through the induction of intracellular ROS production, A549 cells, incubated with different doses of $ZnSO_4$, telmisartan, and ZnTelm for 24 h, were assessed using the oxidant-sensitive dye H_2DCFDA. The compounds have the potential to induce ROS production in A549 cells in a concentration-dependent manner as shown in Fig. 4a. These data agree with previous results: telmisartan triggers ROS formation in leukemia cell lines [19] and $ZnSO_4$ in mammary adenocarcinoma [20]. From Fig.4a, it can be seen that

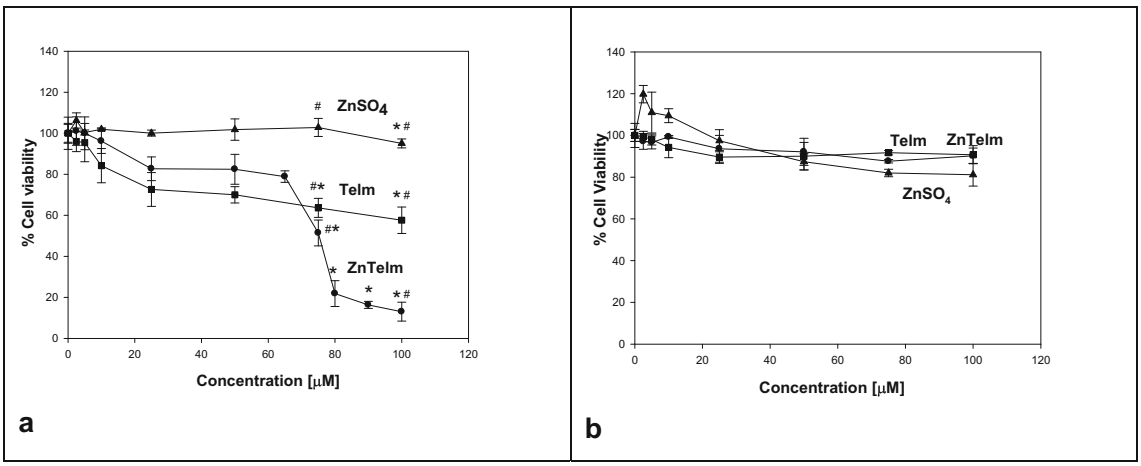

Fig. 3 Viability of the A549 (**a**) and MRC-5 (**b**) cell lines with successive additions of $ZnSO_4$, telmisartan, and ZnTelm for 24 h. Each result (performed in triplicate) represents the mean ± standard error of the mean (SEM) of three independent experiments. Cell viability was calculated as the percentage of live cells compared to the control (% basal). *Statistically significant values between A549-treated cells and control ($p < 0.05$). #Statistically significant values between $ZnSO_4$, telmisartan and ZnTelm at the same concentration ($p < 0.05$)

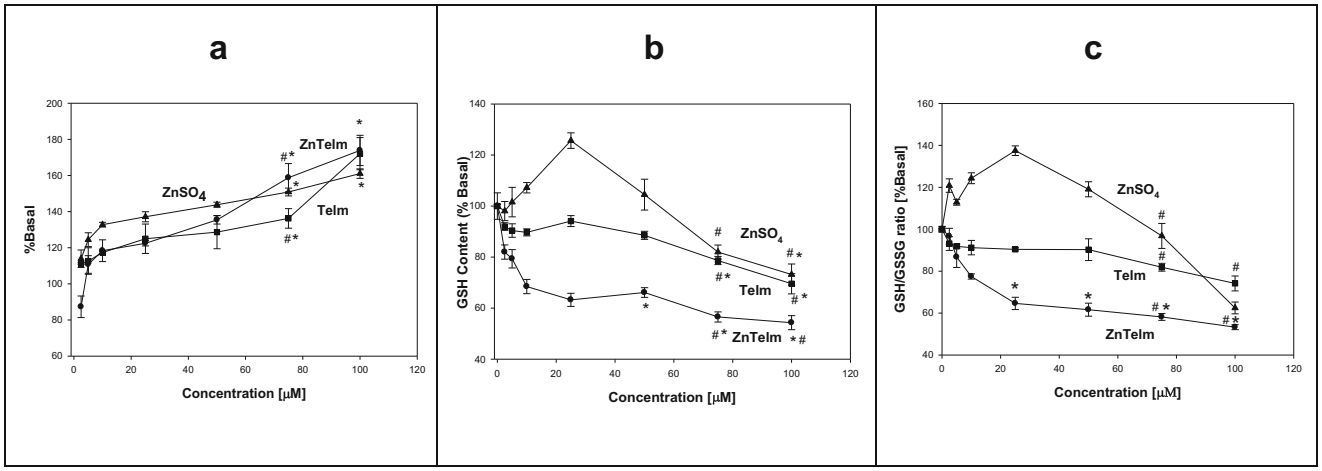

Fig. 4 Effects of 0–100 μM $ZnSO_4$, telmisartan, and ZnTelm on ROS production (**a**), GSH level (**b**), and GSH/GSSG ratio (**c**) in A549 cell line. Each result represents the mean ± standard error of the mean (SEM) of three independent experiments and each was performed by triplicate. *Statistically significant values between A549-treated cells and control ($p < 0.05$). #Statistically significant values between $ZnSO_4$, telmisartan, and ZnTelm at the same concentration ($p < 0.05$)

in the treatment of ZnTelm at the IC_{50} dose (75 μM), intracellular ROS levels were significantly higher compared to the same concentration of telmisartan. These data suggest that the coordination of Zn^{2+} with telmisartan generating a single molecule would enhance the disruptive action on the cellular redox state.

Metal complexes can interfere in cellular redox chemistry in several ways: directly through metal or ligand redox centers or indirectly by binding to biomolecules involved in cellular redox pathways [21]. At physiological pH value, the ligand is deprotonated bearing a negative charge. In the complex, two ligands neutralize their electrical charge with the Zn(II) ion and facilitate the transport of the lipophilic complex through the cell membrane by passive diffusion interacting non-covalently with proteins or intercalating into the DNA molecule. Besides, metal complexation confers more rigidity to the ligand favoring DNA intercalation, so a positive synergic effect may occur.

To determine whether ROS increment could result in the natural antioxidant glutathione (GSH) depletion and cell death, GSH levels have been measured. GSH, a tripeptide non-protein thiol compound, acts as a defense system against oxidative stress that oxidized to (GSSG). Therefore, GSH/GSSG ratio could be a good signal of oxidative stress generation. The method developed by Hissin and Hilf [11] has been used to determine GSH and GSSG levels. Treatment with telmisartan and ZnTelm caused downregulation of GSH levels in a dose–response manner; however, ZnTelm decreased the cellular GSH contents and the GSH/GSSG ratio at lower concentrations than telmisartan (Fig. 4b and c, respectively). This decline is concomitant with ROS generation by both compounds hence it can be assumed that free radicals production plays a key role in the toxic effects of the commercial drug and the complex. On the other hand, it was shown that the exposure to large concentrations of exogenous zinc induces cytotoxicity in A549 cells (IC_{50} 287.1 μM) having low impact in the viability at 50 μM and 100 μM. However, at these low concentrations, the indicators of oxidative stress are increased [22].

To establish if apoptosis is the mechanism of target dell death by ZnTelm, acridine orange/ethidium bromide double staining assay was performed. AO penetrates the cells, and due to its intercalation with DNA, green fluorescence emission in living cells was observed. Furthermore, it acted as a weak base in active acidic lysosomes exhibiting red fluorescence which can be observed as red granules [23]. The red fluorescence emission of the intercalating agent ethidium bromide occurred with altered (late apoptotic or necrotic) cell membranes. Hence, four different cellular stages could be distinguished with this technique: bright green nuclei, live cells (control); orange irregular nuclei displaying apoptotic bodies, early apoptotic cell; orange to red nuclei with highly fragmented chromatin, late apoptotic cells; and red fluorescence, necrotic cells. The treatment with 75 μM $ZnSO_4$ (IC_{50} of the complex) did not produce cellular alteration (Fig. S2). Cells treated with 75 μM telmisartan induced ca. 39% cellular death with 6% found to be early apoptosis, 17% late apoptosis and 21% of necrosis (Fig. 5; Table S2). ZnTelm produced *ca.* 52% of cellular death, 30% of cells in early apoptosis, 21% late apoptosis, and 2% of necrosis. Moreover, ZnTelm generated red granules corresponding to lysosomes, which are involved in the initiation of apoptosis [24]. Previous studies showed that telmisartan mediates low frequencies of early and late apoptotic events against renal cancer cells at large concentrations (100 and 200 μM) [25]. Granular apoptotic bodies, membrane blebbing, and cell shrinkage, indicating apoptosis, were observed in response to ZnTelm treatment in A549 cells as the main morphological changes. As a whole, our data suggest that the main mechanism of A549 cell death produced by ZnTelm treatment could be early apoptosis. In contrast, the treatment with telmisartan mainly suggests a necrotic cell death mechanism.

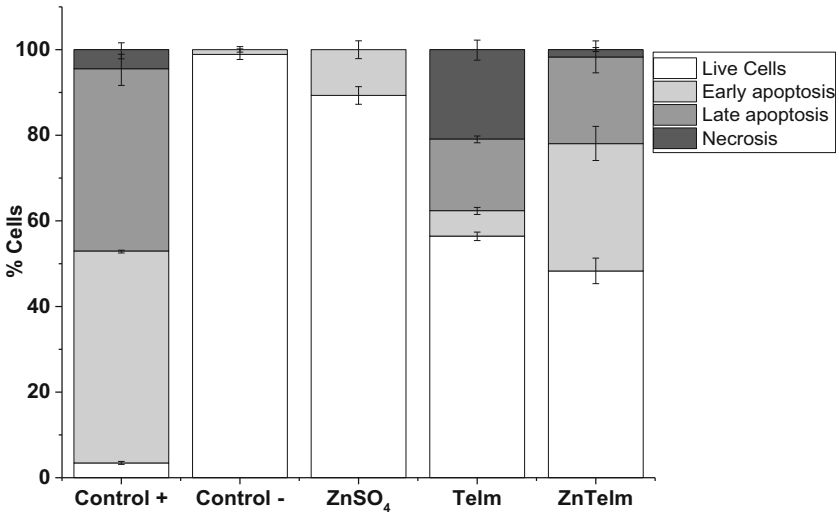

Fig. 5 Plot of percentage of live A549 cells and cell death stages. Cell death stage was analyzed by counting AO/BE–stained cells

During apoptosis (programmed cell death), a group of intracellular proteases, caspases, are responsible for a proteolytic degradation of a host of intracellular proteins into apoptotic bodies. The protein expression of apoptosis regulators, including Bax and caspase-3 (pro-apoptotics) and Bcl-XL (antiapoptotic), was measured by Western blotting. The expression of caspase-3 and Bax upon incubation with ZnTelm increased with respect to the control group, telmisartan, and $ZnSO_4$, while the expression of Bcl-XL decreased (Fig. 6), in accord to the results obtained by AO/BE staining: ZnTelm promotes apoptosis in A549 cells.

It can be concluded that the combination between Zn(II) and telmisartan with proven anticancer properties may cause synergetic effects to potentiate the anticancer activity in the complex. The mechanism results from oxidative stress induced apoptotic signaling as a consequence of an increase in ROS generation and depletion in natural antioxidants.

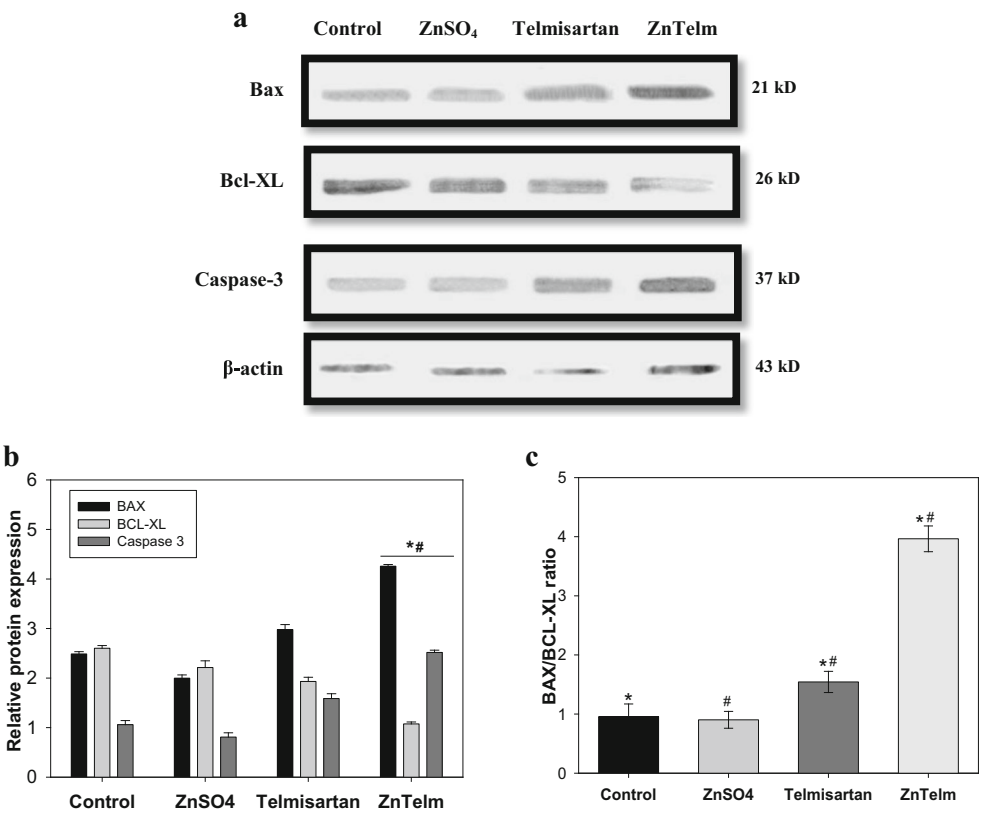

Fig. 6 **a** Western blotting of the expression levels of Bax, Bcl-XL, and Caspase 3 proteins in A549 cells incubated with 75 μM of $ZnSO_4$, telmisartan, and ZnTelm (Internal control: β-Actin), in three independent experiments. **b** Densitometric quantification of relative protein levels. **c** Bax/Bcl-XL ratio. *Values statistically significant between A549-treated cells and control ($p < 0.05$). #Values statistically significant between telmisartan, $ZnSO_4$, and ZnTelm at the same concentration ($p < 0.05$)

Interactions with BSA

The major protein in plasma, albumin, is able to bind and transport a wide diversity of compounds with high affinity as a reversible process [26, 27]. The fluorescence measurements for the determination of the interaction of some organic molecules to proteins can give information on its mechanism, binding constants, and binding sites.

The measurement of the fluorescence intensities before and after the addition of different amounts of BSA to telmisartan and ZnTelm allowed the determination of their interactions. This procedure was chosen because at 280 nm (λ_{ex} BSA), the emission spectra for both telmisartan and ZnTelm were very significant (due to the presence of biphenyl and benzimidazole groups) [28] and the spectra overlapped with that of BSA. Figure S3 shows the regular decrease of the intrinsic fluorescence of telmisartan and ZnTelm with successive BSA additions, indicating the interaction with the compounds. The maximum emission wavelengths of telmisartan and ZnTelm at pH 7.4 are located at 360 nm. The maximum fluorescence emission of telmisartan-BSA (375 nm) and ZnTelm-BSA (380 nm) shifted to the red (Fig. S3), suggesting an increase of the hydrophilic microenvironment around the benzimidazole group.

Data analysis, at 298 K and 310 K, was performed with the Stern-Volmer equation:

$$F_0/F = 1 + k_q\tau_0[Q] = 1 + K_{SV}[Q] \quad (1)$$

where F_0 and F are the fluorescence intensities before and after quencher addition, respectively, K_q is the bimolecular quenching constant, [Q] is the concentration of the quencher, τ_0 is the half-life of the fluorophore without quencher, and K_{sv} is the quenching constant of Stern-Volmer. The maximum (F) and the initial (F_0) fluorescence values of telmisartan and ZnTelm were obtained from the wavelength of maximum fluorescence shifts of the deconvolved spectra. Therefore, from Eq. 1, K_{sv} can be determined from the linear regression of the plot F_0/F vs. albumin concentration (Fig. S4). Both graphs show linearity for all tested BSA concentrations, indicating that the quenching could be static or dynamic. The calculated values of K_{sv} (Table 1) show that these constants decrease with the increment of the temperature, evidencing that the possible mechanisms of interaction are static in both cases.

The equilibrium between free and bound small molecules upon binding to some sites of the protein is described by the Scatchard equation:

$$\log[(F_0-F)] = \log K_a + n\log[Q] \quad (2)$$

that allow the calculation of the binding constant (K_a) and the number of binding sites (n) (Fig. S5; Table 1). From this evaluation, only one binding site for the interaction of both telmisartan and ZnTelm to BSA was determined. In general, the value of K_a for the interaction compound-albumin must be high enough to ensure the transport and distribution throughout the body, but simultaneously, low enough to allow the compound to be released to reach its goal. The optimal K_a range is between 10^4 and 10^6 M^{-1} [29]. Therefore, our results (K_a ca. 10^4 M^{-1}) confirmed that the carrier BSA could bond and transport the present compounds.

The type of interactions existing between the ligand and the complex with BSA were evaluated from the thermodynamic parameters (ΔH, ΔS, and ΔG). The enthalpy (ΔH) and the entropy (ΔS) changes can be estimated using the van't Hoff eq. (3)

$$\ln K_a = (-\Delta H^o/RT) + \left(\Delta S^0/R\right) \quad (3)$$

where R is the gas constant. The free energy change, ΔG^o, was calculated from eq. (4):

$$\Delta G^o = \Delta H^o - T\Delta S^o \quad (4)$$

The negative sign for ΔG (Table 2) suggests that complex formation with BSA is spontaneous. Different types of interaction could be involved in the process of protein association, and they could be evaluated considering the magnitude of the enthalpy and entropy changes. Positive changes of both parameters indicated hydrophobic interactions; negative values indicated that Van der Waals forces and hydrogen bonding bonds are acting between the compound and the protein and $\Delta H < 0$ and $\Delta S > 0$ are indicative for electrostatic interactions [30]. Therefore, from Table 2, it can be seen that BSA-Telm binds through hydrophobic interaction ($\Delta H > 0$ and $\Delta S > 0$) probably due to the stacking generated by the aromatic rings of BSA (tryptophan, phenylalanine, and tyrosine) and the aromatic rings of the ligand. The stabilization of the bond through hydrophobic interactions between telmisartan and

Table 1 K_{sv}: Stern-Volmer constant, K_q: quenching rate constant, and K_a: binding constant, for BSA interaction with telmisartan and ZnTelm

Compounds	T (K)	K_{sv} ($\times 10^4$) (L mol^{-1})	r^2	K_q ($\times 10^{12}$) (L mol^{-1} s^{-1})	K_a ($\times 10^4$) (L mol^{-1})	Number of binding sites
Telmisartan	298	61.50 ± 0.03	0.9985	61.5 ± 0.03	290 ± 0.06	1.18 ± 0.02
	310	51.38 ± 0.04	0.9989	51.38 ± 0.04	201 ± 0.03	1.17 ± 0.04
ZnTelm	298	12.68 ± 0.05	0.9973	12.68 ± 0.05	11.09 ± 0.09	0.98 ± 0.03
	310	7.41 ± 0.07	0.9894	7.41 ± 0.07	5.65 ± 0.02	0.97 ± 0.04

Table 2 Thermodynamic parameters for the interactions of BSA with telmisartan and ZnTelm

Compounds	ΔH (KJ mol^{-1})	ΔS (J mol^{-1})	ΔG (KJ mol^{-1})
Telmisartan	23.3	45.48	− 36.85 (298 K) − 37.4 (310 K)
ZnTelm	− 43.10	− 48.12	− 28.76 (298 K) − 28.19 (310 K)

human serum albumin (HSA) has previously been reported [31]. On the contrary, the negative values of ΔH and ΔS for the ZnTelm-BSA complex are indications that van der Waals forces and hydrogen bonding are acting in the binding reaction.

Discussion

Metals ions, in particular, transition metals, offer a diversity of properties when they bind to organic ligands. Cisplatin and other platinum derivatives are coordination complexes used successfully as anticancer drugs but display serious side effects, general toxicity, and drug resistance. As a consequence, new coordination compounds with promising activities on the therapy for carcinogenic diseases have been designed. It is known that a deficiency in the homeostasis of zinc metabolism can cause the progression of oncogenic processes [32] and that telmisartan is an effective drug in lowering blood pressure with a demonstrated inhibitory effect on lung cancer cell proliferation [3]. Therefore, we hypothesized that a coordination compound between Zn(II) and this medication could improve the anticancer activity of the commercial antihypertensive drug. The ZnTelm complex has been successfully synthesized, and the characterization has been performed by means of spectroscopic techniques.

The anticancer effects of telmisartan in A549 cells have previously been reported [2, 18]. We found that ZnTelm showed a significantly high potency with a lower value of IC_{50} and no cytotoxic effects against MRC-5 cell line were observed. The treatment with Zn(II) ions up to 100 μM did not decrease the cell viability in agreement with other reports [33, 34]. These findings clearly indicated that the structural modification of telmisartan by Zn(II) complexation ameliorated the anticancer effect in the tested human lung cancer cells with selectivity. The cellular damage induced by oxidative stress is an essential factor for the design of novel cancer-targeting drugs. Telmisartan stimulated cellular ROS production [4], and ZnTelm triggered higher levels of ROS. Increased ROS generation together with decreased GSH (and GSH/GSSG) levels are important contributions on the mechanism of cell death by oxidative stress. The couple GSH and GSH/GSSG ratio for the complex showed a higher depletion in lung cancer cells. Moreover, the induction of apoptosis can be activated by two mechanisms: the death receptor signaling that is indicative of the extrinsic pathway and mitochondrial alterations that describe the intrinsic pathway. The intrinsic pathway followed by caspase activation is controlled by the Bcl-2 (pro- and antiapoptotic) protein family [35]. The results revealed that ZnTelm had a greater effect in the early phase of apoptosis while telmisartan showed necrotic cells at the same concentration. To investigate the basic molecular mechanisms of apoptosis induced by ZnTelm in A549 cells, the expression levels of the pro-apoptotic Bax and antiapoptotic Bcl-XL proteins as well as the death executor caspase-3 were determined. Telmisartan slightly increased the Bax expression and caspase-3 activation as shown in other reports [36, 37]. However, ZnTelm treatment showed a strong increment of both proteins. Regarding Bcl-XL expression, telmisartan dropped off the level while in ZnTelm group, a higher decrease was observed. These results indicated that intrinsic pathways involved in cell induced apoptosis by ROS generation mediated the anticancer effects of ZnTelm. This apoptotic pathway triggered by mitochondrial dysfunctions has previously been determined for Zn-azilsartan and Zn-Losartan complexes [38, 39]. Treatment with 75 μM $ZnSO_4$ did not alter Bax, Bcl-XL and caspase-3 protein levels in cells. Furthermore, it has been reported that telmisartan cause cell death by overlapping autophagy and apoptosis in adult T cell leukemia cells [19] and in A549 cells [4]. The persistent autophagy, which depletes the organelles and proteins, can lead to a caspase-independent form of cell death and the mechanism of autophagy can often be observed in cells producing necrosis as a result. These findings suggested that necrosis, autophagy, and apoptosis may coexist, and the relative contributions of each process can guide the trajectory of cell death [40]. In the A549 cell line, telmisartan at the same concentration of ZnTelm produced apoptosis and also necrosis and the apoptotic proteins did not significantly increase in comparison to those of the complex [41]. Moreover, it has been reported that a moderate lysosomal rupture induces apoptosis, while severe lysosomal damage produces necrosis [42]. Intact lysosomes are observed on fluorescence assays by the red granular cell distribution (AO staining) upon exposition of cells to 75 μM Zntelm (but not with telmisartan), and this is a possible mechanism of the apoptotic processes shown by the complex (Fig. S6). While "mol-to-mol" comparisons between ligand, metal, and complex are difficult to be performed for compounds with a 2:1 stoichiometry, an additive effect where the behavior of the complex is equivalent to that of the metal plus the ligand (in a double ratio) can be ruled out. The comparisons of the effects of 2 mol of ligand plus 1 mol of metal showed differences in ROS generation (antagonistic effect) and GSH depletion (synergistic effect) and allow us to determine that the differences between the effects of the components separately and the metal complex are significant.

Moreover, the metal complex has the advantage that by supplying equal concentrations of the ligand and the complex (e.g., 50 μM), twice as much telmisartan can be incorporated and that would eventually reduce the side effects of the drug alone. Furthermore, the neutral coordination complex could be a better carrier of the anionic telmisartan (deprotonated at physiological pH values).

Conclusion

To provide other therapeutic properties to commercial drugs, we have prepared and characterized the Zn(II) complex coordinated to the antihypertensive drug telmisartan, ZnTelm. The complex confers marked anticancer effects, which induces oxidative stress with an intrinsic apoptotic pathway including regulation of proteins related to apoptosis improving the antiproliferative action of the parent drug. In addition, the complex did not affect the viability of normal fibroblasts, which accounts for the specificity of the compound. BSA could transport and deliver the complex and telmisartan (with low affinity) through different mechanisms of binding. In conclusion, we have shown that the ZnTelm complex designed by structural modification of telmisartan by Zn(II) complexation enhanced the biological properties of the antihypertensive drug and can be evaluated for its potential as new metal-based drug for the treatment of cancer.

Funding Information The following grants supported this work: UNLP [X/736], CONICET [PIP 0611], CICPBA and ANPCyT (PICT-2016-1814) Argentina. VRM is CONICET fellowship holder, and EGF and PAMW are research fellows of CONICET and CICPBA, respectively.

Compliance with Ethical Standards

Conflict of Interest The authors declare that they have no conflict of interest.

References

1. Burnier M (2009) Telmisartan: a different angiotensin II receptor blocker protecting a different population? J Int Med Res 37:1662–1679. https://doi.org/10.1177/147323000903700602
2. Li J, Chen L, Yu P, Liu B, Zhu J, Yang Y (2014) Telmisartan exerts anti-tumor effects by activating peroxisome proliferator-activated receptor-γ in human lung adenocarcinoma A549 cells. Molecules 19:2862–2876. https://doi.org/10.3390/molecules19032862
3. Zhang S, Wang Y (2018) Telmisartan inhibits NSCLC A549 cell proliferation and migration by regulating the PI3K/AKT signaling pathway. Oncol Lett 15:5859–5864. https://doi.org/10.3892/ol.2018.8002
4. Rasheduzzaman M, Moon JH, Lee JH, Nazim UM, Park SY (2018) Telmisartan generates ROS-dependent upregulation of death receptor 5 to sensitize TRAIL in lung cancer via inhibition of autophagy flux. Int J Biochem Cell Biol 102:20–30. https://doi.org/10.1016/j.biocel.2018.06.006
5. Livingstone C (2015) Zinc: physiology, deficiency, and parenteral nutrition. Nutr Clin Pract 30:371–382. https://doi.org/10.1177/0884533615570376
6. Marreiro D, Cruz K, Morais J et al (2017) Zinc and oxidative stress: current mechanisms. Antioxidants 6:1–24. https://doi.org/10.3390/antiox6020024
7. Ho E, Ames BN (2002) Low intracellular zinc induces oxidative DNA damage, disrupts p53, NF B, and AP1 DNA binding, and affects DNA repair in a rat glioma cell line. Proc Natl Acad Sci 99:16770–16775. https://doi.org/10.1073/pnas.222679399
8. Ho E (2004) Zinc deficiency, DNA damage and cancer risk. J Nutr Biochem 15:572–578. https://doi.org/10.1016/j.jnutbio.2004.07.005
9. Zhao JNA, Mi L, Hu J, Hou H, Fan Y (2008) Cation exchange induced tunable properties of a nanoporous octanuclear Cu(II) wheel with double-helical structure. J Am Chem Soc 130:15222–15223. https://doi.org/10.1021/ja8007227
10. Lee HW, Kang LH, Yoo CL, et al (2010) The new telmisartan zinc salt and the preparation thereof. Patent WO/2010/053233 1–15
11. Hissin PJ, Hilf R (1976) A fluorometric method for determination of oxidized and reduced glutathione in tissues. Anal Biochem 74:214–226. https://doi.org/10.1016/0003-2697(76)90326-2
12. Bradford MM (1976) A rapid and sensitive method for the quantitation of microgram quantities of protein utilizing the principle of protein-dye binding. Anal Biochem 72:248–254. https://doi.org/10.1016/0003-2697(76)90527-3
13. Wu X (2015) Dual AO/EB staining to detect apoptosis in osteosarcoma cells compared with flow cytometry. Med Sci Monit Basic Res 21:15–20. https://doi.org/10.12659/MSMBR.893327
14. Islas MS, Martínez Medina JJ, López Tévez LL et al (2014) Antitumoral, antihypertensive, antimicrobial, and antioxidant effects of an octanuclear copper(II)-telmisartan complex with an hydrophobic nanometer hole. Inorg Chem 53:5724–5737. https://doi.org/10.1021/ic500483p
15. Bano S, Mohd A, Aslam A et al (2010) Complexation and mechanism of fluorescence quenching of telmisartan with Y (III) and Nd (III). J Chem Eng Data 55:5759–5765. https://doi.org/10.1021/je100711u
16. Bakheit AHH, Abd-Elgalil AA, Mustafa B et al (2015) Telmisartan. Profiles Drug Subst Excipients Relat Methodol 40:371–429. https://doi.org/10.1016/bs.podrm.2015.01.003
17. Sanjeev Kumar A, Ghosh S, Mehta GN (2010) Efficient and convergent synthesis of telmisartan. Res J Pharm, Biol Chem Sci 1:461–468. https://doi.org/10.3762/bjoc.6.25
18. Godugu C, Patel AR, Doddapaneni R, Marepally S, Jackson T, Singh M (2013) Inhalation delivery of telmisartan enhances intratumoral distribution of nanoparticles in lung cancer models. J Control Release 172:86–95. https://doi.org/10.1016/j.jconrel.2013.06.036s
19. Kozako T, Soeda S, Yoshimitsu M, Arima N, Kuroki A, Hirata S, Tanaka H, Imakyure O, Tone N, Honda S, Soeda S (2016) Angiotensin II type 1 receptor blocker telmisartan induces apoptosis and autophagy in adult T-cell leukemia cells. FEBS Open Bio 6:442–460. https://doi.org/10.1002/2211-5463.12055
20. Provinciali M, Donnini A, Argentati K, di Stasio G, Bartozzi B, Bernardini G (2002) Reactive oxygen species modulate Zn^{2+}-induced apoptosis in cancer cells. Free Radic Biol Med 32:431–445. https://doi.org/10.1016/S0891-5849(01)00830-9
21. Romero-Canelón I, Mos M, Sadler PJ (2015) Enhancement of selectivity of an organometallic anticancer agent by redox modulation. J Med Chem 58:7874–7880. https://doi.org/10.1021/acs.jmedchem.5b00655
22. Kocdor H, Ates H, Aydin S, Cehreli R, Soyarat F, Kemanli P, Harmanci D, Cengiz H, Kocdor MA (2015) Zinc supplementation induces apoptosis and enhances antitumor efficacy of docetaxel in

non-small-cell lung cancer. Drug Des Devel Ther 9:3899–3909. https://doi.org/10.2147/DDDT.S87662
23. Lovelace M, Cahill D (2007) A rapid cell counting method utilising acridine orange as a novel discriminating marker for both cultured astrocytes and microglia. J Neurosci Methods 165:223–229. https://doi.org/10.1016/j.jneumeth.2007.06.009
24. Brunk UT, Neuzil J, Eaton JW (2001) Lysosomal involvement in apoptosis. Redox Rep 6:91–97. https://doi.org/10.1179/135100001101536094
25. de Araújo Júnior RF, Leitão Oliveira ALC, de Melo Silveira RF, de Oliveira Rocha HA, de França Cavalcanti P, de Araújo AA (2015) Telmisartan induces apoptosis and regulates Bcl-2 in human renal cancer cells. Exp Biol Med 240:34–44. https://doi.org/10.1177/1535370214546267
26. Fasano M, Curry S, Terreno E et al (2005) The extraordinary ligand binding properties of human serum albumin. IUBMB Life 57:787–796. https://doi.org/10.1080/15216540500404093
27. Kragh-Hansen U (1981) Molecular aspects of ligand binding to serum albumin. Pharmacol Rev 33:17–53
28. Verdasco G, Martín MA, del Castillo B et al (1995) Solvent effects on the fluorescent emission of some new benzimidazole derivatives. Anal Chim Acta 303:73–78. https://doi.org/10.1016/0003-2670(94)00365-S
29. Topală T, Bodoki A, Oprean L, Oprean R (2014) Bovine serum albumin interactions with metal complexes. Med Pharm Rep 87:215–219. https://doi.org/10.15386/cjmed-357
30. Ross PD, Subramanian S (1981) Thermodynamics of protein association reactions: forces contributing to stability. Biochemistry 20:3096–3102. https://doi.org/10.1021/bi00514a017
31. Li J, Zhu X, Yang C, Shi R (2010) Characterization of the binding of angiotensin II receptor blockers to human serum albumin using docking and molecular dynamics simulation. J Mol Model 16:789–798. https://doi.org/10.1007/s00894-009-0612-0
32. Prasad AS, Beck FWJ, Snell DC, Kucuk O (2009) Zinc in cancer prevention. Nutr Cancer 61:879–887. https://doi.org/10.1080/01635580903285122
33. Zhao WJ, Song Q, Zhang ZJ et al (2015) The kinetic response of the proteome in A549 cells exposed to $ZnSO_4$ stress. PLoS One 10:1–21. https://doi.org/10.1371/journal.pone.0133451
34. Yuan N, Wang Y-H, Li K-J et al (2012) Effects of exogenous zinc on the cellular zinc distribution and cell cycle of A549 cells. Biosci Biotechnol Biochem 76:2014–2020. https://doi.org/10.1271/bbb.120216
35. Kang MH, Reynolds CP (2009) Bcl-2 inhibitors: targeting mitochondrial apoptotic pathways in cancer therapy. Clin Cancer Res 15:1126–1132. https://doi.org/10.1158/1078-0432.CCR-08-0144
36. Wang C, Wang W (2018) Telmisartan induces osteosarcoma cells growth inhibition and apoptosis via suppressing mTOR pathway. Open Life Sci 13:242–249. https://doi.org/10.1515/biol-2018-0029
37. Koyama N, Nishida Y, Ishii T, Yoshida T, Furukawa Y, Narahara H (2014) Telmisartan induces growth inhibition, DNA double-strand breaks and apoptosis in human endometrial cancer cells. PLoS One 9:e93050. https://doi.org/10.1371/journal.pone.0093050
38. Martínez VR, Aguirre MV, Todaro JS, Piro OE, Echeverría GA, Naso LG, Ferrer EG, Williams PAM (2018) Interaction of Zn with losartan. Activation of intrinsic apoptotic signaling pathway in lung cancer cells and effects on alkaline and acid phosphatases. Biol Trace Elem Res 186:413–429. https://doi.org/10.1007/s12011-018-1334-x
39. Martínez VR, Aguirre MV, Todaro JS et al (2018) Azilsartan and its Zn(II) complex. Synthesis, anticancer mechanisms of action and binding to bovine serum albumin. Toxicol in Vitro 48:205–220. https://doi.org/10.1016/j.tiv.2018.01.009
40. Amaravadi RK, Thompson CB (2007) The roles of therapy-induced autophagy and necrosis in cancer treatment. Clin Cancer Res 13:7271–7279. https://doi.org/10.1158/1078-0432.CCR-07-1595
41. Matsui T, Chiyo T, Kobara H et al (2019) Telmisartan inhibits cell proliferation and tumor growth of esophageal squamous cell carcinoma by inducing S-phase arrest in vitro and in vivo. Int J Mol Sci 20:1–14. https://doi.org/10.3390/ijms20133197
42. Zhao M, Antunes F, Eaton JW, Brunk UT (2003) Lysosomal enzymes promote mitochondrial oxidant production, cytochrome c release and apoptosis. Eur J Biochem 270:3778–3786. https://doi.org/10.1046/j.1432-1033.2003.03765.x